Journal of
Materials Chemistry C

Accepted Manuscript

Journal of
Materials Chemistry C

Cite this: DOI: 10.1039/c0xx00000x

ARTICLE TYPE

www.rsc.org/xxxxxx

Sterically Demanded Zinc(II)Phthalocyanines: Synthesis, Optical, Electrochemical, Nonlinear Optical, Excited State Dynamics Studies

Debasis Swain,[a] Radhakant Singh,[a] Varun Kumar Singh,[b] Narra Vamsi Krishna,[b] Lingamallu Giribabu[b,*], Soma Venugopal Rao[a,*]

Abstract

Two novel sterically demanded Zinc phthalocyanines were synthesized and characterized. Their optical and electrochemical properties have been investigated in detail. Emission spectra were recorded in different solvents and the fluorescence yields obtained were in the range of 0.2-0.3 while time-resovled fluorescence data revealed radiative lifetimes of typically few ns. Nonlinear optical (NLO) properties were also evaluated at wavelengths of 600 nm, 640 nm, 680 nm, and 800 nm using picosecond (~1.5 ps) pulses and further studies with femtosecond (~140 fs) pulses at 800 nm, 780 nm were also performed. Two-photon absorption (2PA) and saturable absorption (SA) were the dominant nonlinear asorption mechanmisms observed with ps/fs excitation at different wavelengths in the visible spectral region. NLO coefficients were extracted from ps/fs closed and open aperture Z-scan measurements. Large two-photon absorption cross-sections of ~14000 GM and n_2 values in the range of 1-7×10^{-16} cm^2/W were retreived for these molecules from the ps Z-scan data. The excited state decay dynamics were investigated using degenerate pump-probe experiments with~70 fs pulses near 600 nm. Double exponential fits of the pump-probe data suggested two decay times for both the molecules investigated.

Received (in XXX, XXX) XthXXXXXXXXX 2013, Accepted Xth XXXXXXXXX 2013
DOI: 10.1039/b000

Introduction

Phthalocyanines (Pcs) and their metallo derviatves (MPc) have ascertained extensive applications in several fileds, such as colorants, chemical sensors, electrochromism, catalysts, liquid crystals, nonlinear optics and as sensitizers in photodynamic therapy as well as in dye-sensitized solar cells.[1-8] The wide range of phthalocyanine applications are primarily because of their high molar absorption coefficient ($\varepsilon > 10^5$) in the far end of the visible spectrum, high triplet state quantum yields, long lifetimes, exceptionally high thermal and chemical stability, and rational synthetic routes towards preparation of of these compounds.[9] Phthalocyanines offer great structural flexibility with the possibility of hosting more than 70 different elements in the central cavity. The optical properties of Pcs, of great scientific interest, depend on the solubility as well as aggregation of the macroccyle.[10-11] Owing to the extended π-systems, these complexes show high aggregation tendency in both solution and solid state, less solubility in common organic solvents thus influencing their spectroscopic and photophysical properties and thereby limiting the application potential.[12] Therefore, much efforts have been directed into designing non-aggregated phthalocyanines in order to control their properties. Essentially, aggregation is due to the cofacial association of the highly planar Pc units even at micromolar concentration, which leads to low efficiencies in device applications.[13]

Consequently, if one could get rid of the planarity either by axial ligation of the Pc molecule or use of bulky substituents at peripheral positions of the Pc-molecule, aggregation can be reduced. The most effective way to reduce aggregation is by creating steric crowding over the phthalocyanines macrocycle by use of bulky substituents.[14-17] Based on thermal, photochemical stability, and electrochemical properties phthalocyanines were found to be alternative sensitizers for dye-sensitized solar cell applications.[18] However, because of planarity of the phthalocyanine, macrocycle tends to aggregate at micormolar concentration and results in low efficiency of the device. Recently, we have successfully introduced bulky substituents at peripheral positions of phthalocyanine macrocycle and designed several efficient sensitizers for dye-sensitized solar cell applications.[19-22] This approach gave highly soluble and non-aggregated Pc derivatives in dilute solution as well as in the solid state. Phthalocyanines are proper choice for effectively harvesting red light due to their strong Q band light absorption properties near 700 nm.Thus,phthalocyanine-sensitized solar cells for use as photovoltaic window transmit part of the visible light and harvest in the red/near-IR part of the spectrum.[23] MPc's are characterized by intense B- and Q-bands centered near 350 and 670 nm, respectively. Strong absorbance in the far red region of the UV/vis spectrum was thus retained upon introduction of the fluorous peripheral substituents.[24]

There have been several novel Pc-based sensitizers reported, including efforts from our group, and explored their interesting nonlinear optical (NLO) properties.[25-32] Several modifications such as substituents on the central metal core, peripheral attachments, incorporation into graphene, doping with polymer, preparing nanoparticles etc.[33-42] were embarked upon with the intention of understanding the structure-property relationship towards tailoring their NLO properties. However, the significant aspects missing amongst these studies are (a) spectral dependence (dispersion studies) of the optical nonlinearity (b) time resolution of the optical nonlinearity (c) pulse width dependent studies. Nonlinear absorption (NLA) studies with nanosecond (ns) pulses (in solution and doped in polymers/glasses) will assist identification materials for optical limiting applications. For such applications time-response of the nonlinearity is not important. NLA studies with

[a]Advanced Centre of Research in High Energy Materials **(ACRHEM),** University of Hyderabad, Prof. C.R. Rao Road, Hyderabad 500046, Andhra Pradesh, India
[b]Inorganic and Physical Chemistry Division, Indian Institute of Chemical Technology, Hyderabad 500 007, India

*Corresponding author e-mail: **svrsp@uohyd.ernet.in, or soma_venu@yahoo.com**; **giribabu@iict.res.in**

† Electronic Supplementary Information (ESI) available: Emission and lifetime spectra of Pc-1 & Pc-2 in different solvents, ESI-MS spectrum of Pc-1 and Pc-2. Open and closed aperture data of Pc-1 and Pc-2 with ~140 fs pulses, summary of all NLO coefficients obtained from this study.

picosecond (ps)/femtosecond (fs) pulses facilitates discovering suitable saturable absorbers for modelocking aplications in ultrafast lasers. Nonlinear refractive index studies with ps/fs pulses will provide information of material properties useful for signal processing, all-optical switching applications. Desired characteristics for applications include small linear absorption, low nonlinear absorption, and strong nonlinear refractive index with sufficiently fast repsonse (ps/fs time scales). All the above mentioned three features are indispensable for identifying the practical applications of any NLO material. Herein, we have designed and prepared two sterically hindered Zn-Pcs by introducing 3,4-dimethoxy (**Pc-1**) and 2,6-dimethoxy (**Pc-2**) phenyl groups at the peripheral positions of Pc-molecule. The intriguing structure-property relationship between the structure and NLO properties has been studied at different wavelengths of the visible region. We have also performed detailed studies of their optical, electrochemical, and emission properties in different solvents.

Experimental Section

Materials

3,4-dimethoxyphenylboronic acid, 4,5-dicholorophthalonitrile, 2,6-dimethoxy phenol, potassium phosphate tribasic, 1-pentanol, o-tritolylphosphine, 1,8-diazabicyclo[5.4.0] undec-7-ene (DBU) and Palladium(0) tetrakis(triphenylphosphine) were purchased from Sigma Aldrich and were used as such. All the solvents *viz.*, dichloromethane, tetrahydrofuran, dimethylsulfoxide, N,N-dimethylformamide, toluene, methanol, chloroform, n-haxane were obtained from SD Fine chemicals Limited, India and were dried before further use.[43] Zinc Acetate and potassium carbonate were purchased from Qualigens Chemicals Ltd, India.

Instrumentation

Absorption spectra were recorded with a Shimadzu UV-3600, UV-Visible-NIR spectrophotometer. Steady-state fluorescence spectra were recorded using a Fluorolog-3 spectrofluorometer (Spex model, Jobin Yvon) for solutions with optical density at the wavelength of excitation (λ_{ex}) ≈0.05. Fluorescence quantum yields (ϕ) were estimated by integrating the fluorescence bands zinc *tert*-butyl phthalocyanine (ϕ=0.37 in benzene).[44] Fluorescence lifetime measurements were carried on a picosecond time-correlated single photon counting (TCSPC) setup (FluoroLog3-Triple Illuminator, IBH Horiba Jobin Yvon) employing a picosecond light emitting diode laser (NanoLED, λ_{ex}= 670 nm) as excitation source. The decay curves were recorded by monitoring the fluorescence emission maxima of the phthalocyanine macrocycle (λ_{em}= 700 nm). Photomultiplier tube (R928P, Hamamatsu) was employed as the detector. The lamp profile was recorded by placing a scattered (dilute solution of Ludox in water) in place of the sample. The width of the instrument function was limited by the full width at half maximum (FWHM) of the excitation source, ~635 ps at 670 nm. Decay curves were analyzed by nonlinear least-squares iteration procedure using IBH DAS6 (version 2.3) decay analysis software. The quality of the fits was judged by the χ^2 values and distribution of the residuals.

Electrochemical measurements were performed on a PC-controlled CH instruments model CHI 620C electrochemical analyzer. The experiments were performed on 1 mM phthalocyanine solution in CH_2Cl_2 solvent at scan rate of 100 mV/s using 0.1 M tetrabutyl ammonium perchlorate (TBAP) as supporting electrolyte. The working electrode is glassy carbon, standard calomel electrode (SCE) is reference electrode and platinum wire is an auxiliary electrode. After a cyclic voltammogram (CV) had been recorded, ferrocene was added, and a second voltammogram was measured. The optical thin layer electrochemical studies were carried on Maya 2000 Ocean Optics software using DT-MINI-2-GS, UV-VIS-NIR LIGHTSOURCE. ^{1}H NMR spectra were recorded in $CDCl_3$ solutions on AVANCE 300 MHz spectrophotometer using TMS as standard. FT-IR spectra (KBr pellets) were recorded on a Perkin Elmer Spectrophotometer. Mass spectra were acquired using ElectroSpray Ionization (ESI) method, operated in positive ion mode using m/z range 100-2000.

NLO and pump-probe studies

All the experiments were performed with samples dissolved in dichloromethane (DCM) and placed in 1-mm glass cuvettes. Ps laser pulses from a regenerative amplifier (Picosecond Legend, Coherent), from which we obtained 1 kHz amplified pulses of ~1.5 ps, with a maximum output energy of ~2.0 mJ. The ps Z-scan[45] measurements were performed at wavelengths of 600 nm, 640 nm, 680nm, and 800 nm. The laser source was a Ti:sapphire laser system (picosecond LEGEND, Coherent) delivering nearly transform- limited pulses of ~1.5ps duration and repetition rate of 1 kHz. The pulse duration was determined by external autocorrelation technique, by using 2 mm thick BBO crystal in non-collinear geometry. The pulses other than 800nm were derived from an optical parametric amplifier (Light conversion, TOPAS). A 200 mm focal length lens was used to focus the beam and the sample is scanned along the laser beam axis direction (Z). The degenerate pump-probe experiments were carried out at 600 nm using ~70 fs pulses from an optical parametric amplifier which was pumped by ~40 fs pulses from an amplifier (Ultrafast Legend, Coherent). Pump-probe power ratios were maintained in the range of 40-50. The probe diameter was <1 mm and was aligned such that it always within the pump diameter of ~3 mm. Data was acquired through the combination of a photo-diode and lock-in amplifier. Complete details of both these experiments are detailed in some of our earlier works.[46-49]

Fs laser pulses for Z-scan studies were obtained from an oscillator (Chameleon, Coherent Inc.) that delivered ~140 fs, 80 MHz pulses at 800 nm. A quartz cuvette (1-mm thick) containing the sample solution was traversed in the focusing geometry enabled by an achromat lens of 100 mm focal length. The beam waist ($2\omega_0$) at focal plane was estimated to be ~40 μm [FW($1/e^2$)M] with a corresponding Rayleigh range (Z_r) of ~1.6 mm ensuring the validity of thin sample approximation. Typically <30 nJ energy pulses were used for the experiments. The sample was translated using a high resolution stage and the transmitted light was collected using a lens and a power meter (Coherent) combination. An aperture was placed in front of the lens for closed aperture scans and total light was collected during open aperture scans. Several neutral density filters were used to reduce the input intensity before the sample and also the intensity reaching photodiode. The translation stage moved mechanically with a step size of 1mm and corresponding transmittance reading was recorded with the power meter. The NLO properties of **Pc-1** and **Pc-2** in DCM as solvent were studied using the open/closed aperture Z-scan technique in both fs and ps time domains.

Synthesis

4,5-bis(3,4-dimethoxy)phthalonitrile(**1**) : This compound was synthesized by adopting Suzuki coupling reaction.[50]A 100 ml round bottom flask was charged with 4,5-dichlorophthalonitrile (0.32 g, 1.62 mmol), 3,4-dimethoxyphenyl boronic acid (1.0 g, 5.5 mmol), P(o-Tolyl)$_3$ (0.1 g, 0.323 mmol), K_3PO_4 (2.05 g, 9.70 mmol) and then flushed with nitrogen for 15 minutes before the addition of $Pd(PPh_3)_4$ (0.04 g, 0.032 mmol). To this 20 ml of anhydrous 1,4-dioxane was added. The reaction mixture was stirred at 90 ^{0}C for 6 h under nitrogen atmosphere. After cooling to room temperature, the reaction mixture was washed twice with water. The combined organic layers were washed once with water, subsequently dried over anhydrous Na_2SO_4, filtered and concentrated under rotary evaporator. The resultant residue was subjected to silica gel column chromatography and eluted with hexane-ethyl acetate (90/10% v/v) to obtain the desired product as yellow powder. Elemental analysis of Anal.Calcd. For $C_{24}H_{20}N_2O_4$% (400.14): C, 71.99; H, 5.03; N, 7.00. Found: C, 71.95; H, 5.03; N, 6.95.**ESI-MS** (m/z): $C_{24}H_{20}N_2O_4$ [400.14]**:** M^+ 400.**^{1}H NMR** (300 **MHz**, **$CDCl_3$**): δ (ppm) 7.76 (s, 2H), 6.62-6.78 (m, 4H), 6.47 (s, 2H), 3.82 (s, 6H), 3.56 (s, 6H); **FT-IR** (**KBr**) υ_{max} 2928, 2223 (CN), 1254, 1024 cm^{-1}.

Pc-1: A mixture of anhydrous zinc acetate (2.20g, 10 mmol), 4,5-bis(3,4-dimethoxy) phthalonitrile (**1**) (2.0 g, 5 mmol), DBU (catalytic amount) and dry 1-pentanol (5 ml) was refluxed at 150^{0}C for 16 h under nitrogen atmosphere. After cooling, the solution was precipitated by methanol, filtered and dried. The obtained solid materials was subjected to silica gel column chromatography and eluted with dichloromethane. The green colored band was collected and re-crystallized from methanol, to get the

desired compound 70% yield. Elemental analysis of Anal. Calcd. For $C_{96}H_{80}N_8O_{16}Zn$% (1667.09): C, 69.16; H, 4.84; N, 6.72. Found: C, 69.20; H, 4.81; N, 6.75. **ESI-MS** (m/z): $C_{96}H_{80}N_8O_{16}Zn$ [1667.09]: 1664 (M^{3+}), 1687 ($M+Na^+$), **FT-IR (KBr)**υ_{max} 2928, 2840, 1254 and 1024 cm^{-1}. **UV-Vis**: (in DCM, λ_{max}, ε $M^{-1}cm^{-1}$) 688 (84,199), 626 (32,048), 347 (57,018).

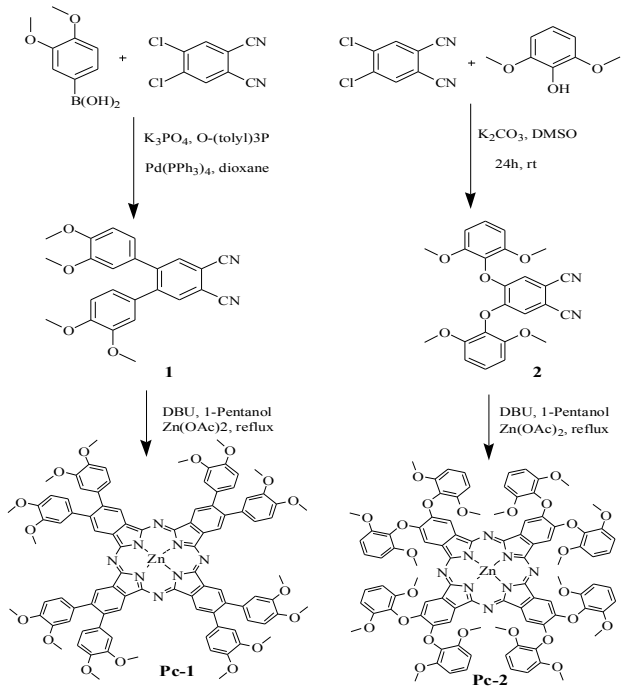

Scheme1 Synthetic routes for **Pc-1** and **Pc-2**

4,5-bis(2,6-dimethoxyphenoxy) phthalonitrile (**2**): 2,6-dimethoxy phenol (3.126 g, 20.30 mmol) and 4,5-dichlorophthalonitrile (1.0 g, 5.076 mmol) were taken in a dry single neck round bottom flask. To this anhydrous K_2CO_3 (7.015 g, 50.76 mmol) and DMF (15 ml) were taken and and stirred at 100ºC under a nitrogen atmosphere for 48 h. The reaction mixture was poured into water and the aqueous layer was extracted thrice with CH_2Cl_2. The organic layer was dried over anhydrous Na_2SO_4, evaporated and the residue was purified by silica gel column chromatography by eluting with Hexane-Ethylacetate (90:10 v/v) to get the desired compound as white solid. Anal. Calcd. For $C_{24}H_{20}N_2O_6$% (432.42): C, 66.66; H, 4.66; N, 6.48. Found: C, 66.70; H, 4.65; N, 7.50. **ESI-MS** (m/z): $C_{24}H_{20}N_2O_6$ [432.42]: (M) 433,**^{1}H NMR (CDCl$_3$,** 300**MHz**): δ (ppm) 7.9 (s, 2H), 6.9 (s, 2H), 6.82(d, J= 8.30 Hz, 4H), 3.78 (s, 12H) **FT-IR** (KBr) υ_{max} 2229 (CN) cm^{-1}

Pc-2: To the mixture of 4,5-bis(2,6-dimethoxy) phthalonitrile (**2**) (2.0 g, 4.6 mmol) and zinc acetate (2.02 g, 9.2 mmol) in 1-pentanol was added DBU in catalytic amount. The reaction mixture was refluxed for 18 h under the nitrogen atmosphere. Then the reaction mixture was cooled to room temperature and precipitated with methanol. The precipitate was filtered, dried and subjected to silica gel column chromatography and eluted with dichloromethane. The green colored band was collected and solvent was evaporated to obtain the desired compound in 73% yield. Elemental analysis of Anal. Calcd. For $C_{96}H_{80}N_8O_{24}Zn$% (1795.09): C, 64.23; H, 4.49; N, 6.24. Found: C, 64.20; H, 4.41; N, 6.25. **ESI-MS** (m/z): $C_{96}H_{80}N_8O_{24}Zn$ [1795.09]: 1793 (M^{2+}), **FT-IR (KBr)**υ_{max} 2930, 2839, 1026 and 1249 cm^{-1}.**UV-Vis**: (in DCM, λ_{max}, ε $M^{-1}cm^{-1}$) 682 (36,078), 614 (6,734), 355 (18,285).

Results and Discussion

Synthesis and characterization

The synthetic routes to new phthalocyanines, **Pc-1** and **Pc-2** are shown in **Scheme 1**. These complexes were prepared by the template of either cyclotetramerization of 4,5-bis(3,4-dimethoxy) phthalonitrile (**1**) or 4,5-bis(2,6-dimethoxyphenoxy) phthalonitrile (**2**) with anhydrous zinc acetate in 1-pentanol at reflux temperature under nitrogen atmosphere in the presence of DBU as a non-nucleophilic base catalyst. Both the phthalocyanines were purified by silica gel column chromatography. and characterized by elemental analysis, Mass, FT-IR, ^{1}H-NMR, UV-Vis., and emission spectroscopy as well as electrochemical techniques. The mass spectra each phthalocyanine consisting of molecular ion peaks at *m/z* 1664 (M^{3+}) and 1793 (M^{2+}), corresponds to the presence of **Pc-1** and **Pc-2**, respectively.

UV-Visible absorption studies

The electronic absorption spectra of **Pc-1** and **Pc-2** revealed characteristic features of the phthalocyanine. They show a low intense Soret band (B band) in the range of 300–400 nm and a relatively intense Q band in the range of 600–800 nm (Fig. 1a and 1b). Strong intensity of this band has been a result of π-π* transitions from the macrocyclic system.

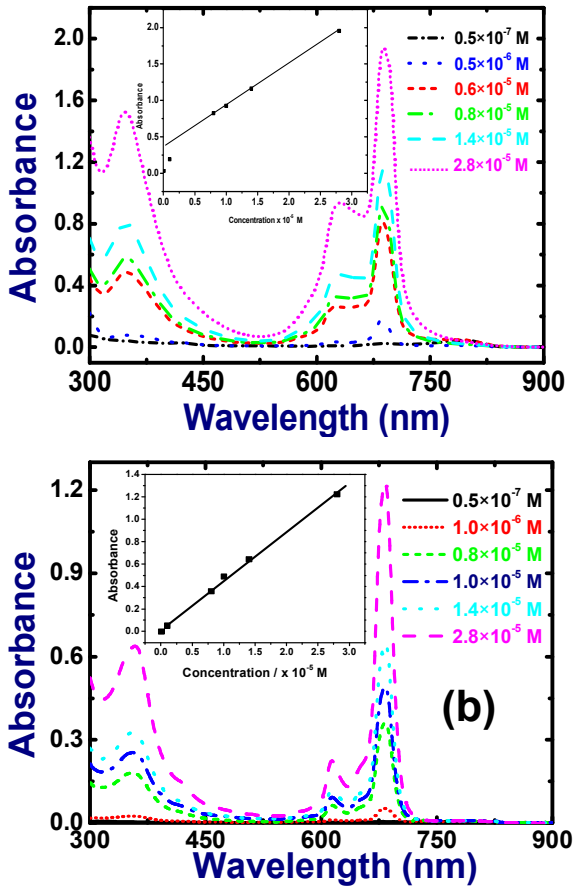

Fig. 1 Absorption spectra of a) **Pc-1** and b) **Pc-2** in CH_2Cl_2 at various concentrations.

UV-visible absorption spectroscopy is a very valuable technique which can be used to study the aggregation phenomena of phthalocyanines in both solution and solid state. The extent and the nature of the molecular packing can also be deduced from the interpretation of UV-visible absorption spectrum (Q band). The insolubility of phthalocyanines in most organic solvents is due to the planarity structure and leads to aggregate by forming π-π stacking. As frequently encountered in most of phthalocyanines, the shoulder on the high energy side of the Q band indicates the presence of aggregated species. The solubility and aggregation problem can be overwhelmed by introducing bulky aryloxy groups at peripheral positions of both phthalocyanines. As anticipated, both phthalocyanines have shown no evidence of aggregation in solution as demonstrated by the sharp unperturbed single Q band, typical of metallated phthalocyanine complexes with D_{4h} symmetry. For example, as shown in Fig. 1b, the absorption spectrum of **Pc-2** depicted a single

sharp Q band at 686 nm in dichloromethane solvent, which is a typical non-aggregated species as evaluated from its position and shape. The concentration dependence of the absorption spectra (insets) of these derivatives was further assessed to prove minimal aggregation. It has been found that both complexes exhibited a monomeric form (*i.e*., no new blue-shifted band due to aggregation) as deduced from the recorded absorption spectra with different concentrations. As shown in Fig. 1b, the appearance of the Q band absorption maxima (*i.e*., shape and position) of **Pc-2** at 686 nm remained unchanged as the concentration increased. It is apparent that molar extinction coefficient remained almost constant indicating almost pure monomeric form, obeying the Beer–Lambert Law in the outlined range of concentrations. Similar non-aggregated properties were also observed in the case of **Pc-1** (Fig. 1a). The introduction of bulky aryloxy groups at the peripheral positions of phthalocyanine did cause any significant shift of the Q band absorption maxima.

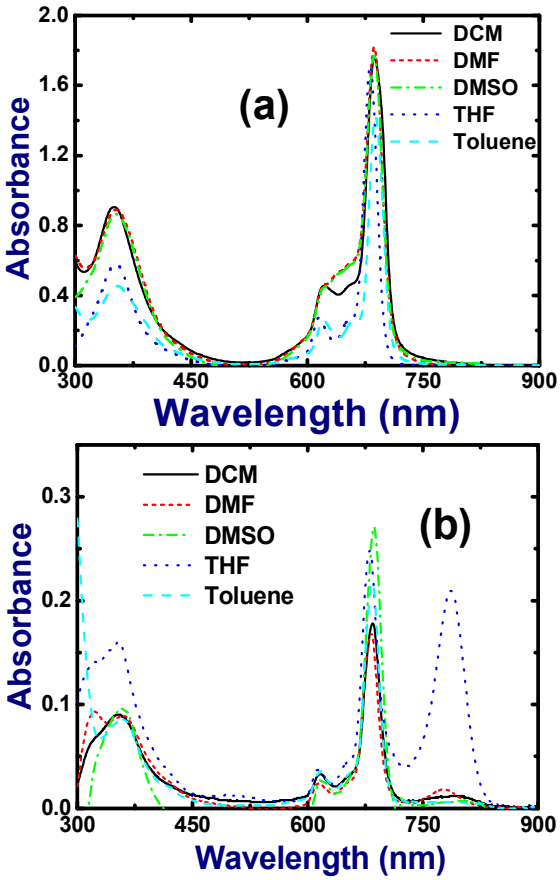

Fig. 2 UV-Visible absorption spectra of **(a) Pc-1 (b) Pc-2** in different solvents.

Figures 2a and 2b illustrate the absorption data of both **Pc-1**and**Pc-2** in various solvents (toluene, THF, DMF, DCM, and DMSO) and the corresponding absorption maxima. The molar extinction coefficients are presented in Table 1. From the data presented in Fig. 2 it is evident that as the solvent polarity increased, the shape and absorption maxima of both B band and Q band did not change. Similar absorption behavior was also observed in **Pc-2**, except in THF and DMSO solvents. In both THF and DMF solvents, Q band was split into two bands at 684 nm and 775 nm, respectively. The split in Q band is probably due to the axial coordination of Zn(II) ion by the solvent molecules.[51]

Electrochemical studies

Cyclic voltammetry and differential pulse voltammetric techniques were adopted to study the redox behavior of both the phthalocyanines. Fig. 3 display cyclic voltammogramme of **Pc-2** and the corresponding data are presented in Table 2. Each of sterically hindered phthalocyanine undergoes two one electron oxidations and two one electron reductions under the experimental conditions employed in this study. All the electrode processes is of either reversible or quasi-reversible reactions. From Fig. 3 and Table 2 it is apparent that the first oxidation of **Pc-2** is shifted cathodically by 150 mV and second oxidation is about 300 mV, when compared to **Pc-1**. This is probable due to more electron releasing groups at the peripheral positions of **Pc-2** than **Pc-1**. The potential difference between the first reduction and first oxidation of **Pc-1** and **Pc-2** in CH_2Cl_2 and 0.1 M TBAP (HOMO-LUMO gap) is 1.61 V and 1.42 V, respectively, a separation within the range of values previously reported for other metallophthalocyanines.[52] Based on well-known electrochemical behavior of phthalocyanine complexes, all couples for **Pc-1** and **Pc-2** are assigned to phthalocyanine ring. The nature of redox couples will also be confirmed using spectro-electrochemical measurements.

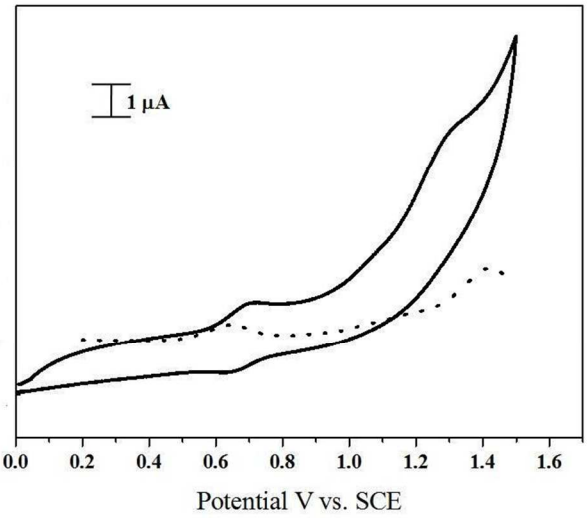

Fig. 3 CV (—) and DPV (----) plots of **Pc-2** in 0.1 M TBAP in DCM

Spectro-electrochemical studies

Spectro-electrochemical studies were performed to monitor changes during redox reactions of these sterically hindered phthalocyanines. Fig. 4a-d shows the spectral changes of **Pc-1** under applied potential. During the controlled potential reduction of **Pc-1** at applied potential of -1.30 V, the intensity of absorption maxima of Q band at 686 nm increases without shift, while new bands at 497 nm and 731 nm are emerged initially. At the same time the B band at 348 nm decrease in intensity and has shifted to 357 nm. The shoulder at 628 nm also decreases in intensity, which indicates disaggregation of the phthalocyanine macrocycle. During this process clear isosbestic points are observed at 373 nm, 555 nm, 672 nm and 703 nm, which clearly indicate that the reduction gives a single product. These changes are typical of the ring-based reduction and assigned to $[Zn^{II}Pc^{-2}]/[Zn^{II}Pc^{-3}]^{-1}$.[53-55] Spectroscopic changes during the controlled potential application at -1.6 V support the further reduction of the monoanionic species confirming the CV assignment of the couple to $[Zn^{II}Pc^{-3}]^{1-}$ / $[Zn^{II}Pc^{-4}]^{2-}$, as shown in Fig. 4b. Both B band and Q band intensities decreased with observation of new band at 730 nm are of characteristic ring reduction. Fig. 4c shows the spectral changes during oxidation process at controlled potential of 0.90 V. The intensity of Q band absorption at 686 nm decreased without shift, while new bands at 526 and 700 nm appeared with increasing intensity. The B band at 348 nm and shoulder at 628 nm decreases in intensity without shift. Clear isosbestic points were recorded at 415 nm, 602 nm and 707 nm. These changes are typical of the ring based oxidation and assigned to $[Zn^{II}Pc^{-2}]/[Zn^{II}Pc^{-1}]^{1+}$ process.[53-55] Spectroscopic changes during the controlled potential application at 1.80 V support the further oxidation of the monocationic species confirming the CV assignment of the couple to $[Zn^{II}Pc^{-1}]^{1+}/[Zn^{II}Pc^{0}]^{2+}$, as shown in Fig. 4d. The band at 348 nm continues to decrease and shoulder at 628 nm has almost diminished. Decrease in intensity of the Q band at 686 nm further supports the ring oxidation process. Clear isosbestic points were recorded at 373, 555, 672 and 703 nm. Fig. 4e-g shows the UV-Vis spectral changes of **Pc-2** during the controlled potential reductions at -1.20 (Fig. 4g) & -1.40 V (Fig. 4h) and

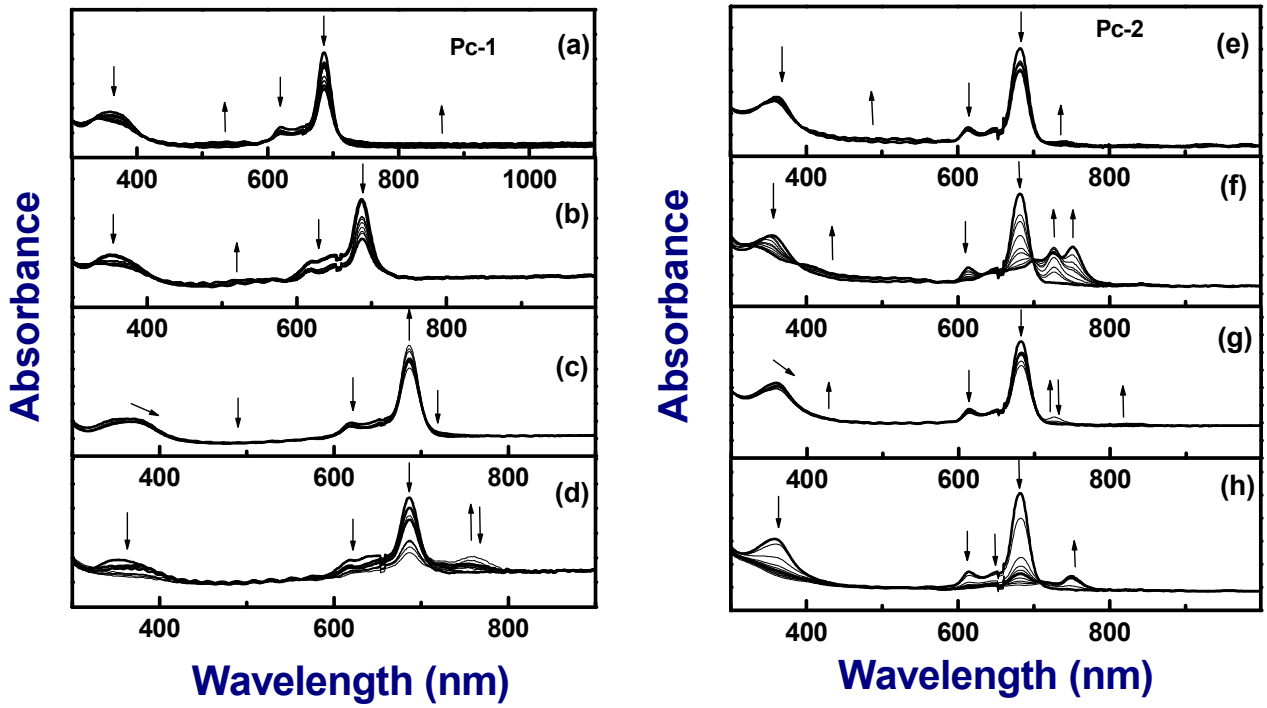

Fig. 4 In-situ UV-Vis spectro-electrochemical changes of **Pc-1.** (a) E_{app}= 0.90 V (b) E_{app}= 1.80 V (c) E_{app}= -1.30 V (d) E_{app}= -1.60 V and **Pc-2** (e) E_{app}= 0.80 V (f) E_{app}= 1.50 V (g) E_{app}= -1.20 V (h) E_{app}= -1.40 V.

oxidations at 0.80 (Fig. 4e) & 1.50 V (Fig. 4f). During applied potential at -1.2 V, the intensity of the Q band at 682 nm decreasing without shift and emerging of new bands at 425 nm and 831 nm and are characteristics of ring based reduction process. Another band at 731 nm emerges and then decreased in intensity. The B band at 362 nm had moved onto 364 nm with decreased intensity. The process is assigned to the couple $[Zn^{II}Pc^{-2}]$ / $[Zn^{II}Pc^{-3}]^{1-}$. During this process, clear isosbestic points were observed at 420, 610 and 700 nm. When the applied potential changed to -1.40 V, both B band at 362 nm and shoulder at 614 nm have completely vanished. In contrast, the intensity of Q band at 682 nm decreases continuously and appears a new band at 752 nm. The process gives isosbestic point at 707 nm. The spectroscopic changes are easily assigned to the reduction of the mono anionic species, $[Zn^{II}Pc^{-3}]^{1-}$ to dianionic species, $[Zn^{II}Pc^{-4}]^{2-}$, Fig 5b. During the controlled potential oxidation at 0.80 V, Fig. 4e, the absorption of the Q band at 682 nm decreases in intensity without shift, while new band at 740 nm appear with increase in intensity. The B band at 362 nm and shoulder at 614 nm decreases in intensity. Clear isosbestic points were recorded at 341, 392, 601 and 707 nm. The changes were assigned to redox couple $[Zn^{II}Pc^{-2}]$ / $[Zn^{II}Pc^{-1}]^{1+}$ species.[53-55] Spectroscopic changes during the controlled potential application at 1.50 V support the further oxidation of monocationic species, $[Zn^{II}Pc,^{-1}]^{1+}$ to $[Zn^{II}Pc,^{0}]^{2+}$ which is evident from the data shown in Fig. 4f. The band at 362 nm and 682 nm and the shoulder at 614 nm have completely vanished. New bands are appeared at 726 nm and 751 nm and are increasing in intensity. Clear isosbestic points were recorded at 331 nm, 389 nm, 584 nm and 700 nm.

Emission Properties

Qualitative evaluation of emission, including quantitative analysis of the fluorescence spectra and determination of the quantum yields (ϕ_f) was performed for **Pc-1** and **Pc-2** in order to understand the effect of peripheral substitution on phthalocyanine macrocycle. The emission spectra of both phthalocyanines were collected by exciting both phthalocyanines at 680 nm. The steady state fluorescence spectra of both the complexes are almost similar except the different emission maxima. As it can be seen in Fig. 5 and Fig. 3, Fig. 4 (supporting material), the emission spectra of **Pc-1** and **Pc-2** were consistent with both the Stokes rule and the rule of mirror symmetry between the absorption and fluorescence bands. The emission properties of **Pc-1**and**Pc-2** in DMSO were evaluated by comparison with those of ZnPc possessing no peripheral substituents. For ZnPc the Stokes shift was small ($\Delta\lambda$ = 7 nm) which confirms that the geometry of the molecule in the singlet excited state S_1 does not differ much from that in the ground state. The Stokes shift in the emission spectra of phthalocyanines possessing peripheral substituents was somewhat greater. Fluorescence quantum yields (ϕ_f) were determined by the comparative method according to the formula[56]

$$\Phi Sample = \frac{FSample \times Abs.Standard}{FStandard \times Abs.Sample} \times \Phi Standard$$

where ϕ_{Sample} is the fluorescence quantum yield of sample; $\phi_{f,Standard}$ is fluorescence quantum yield of the standard; F_{sample} is fluorescence intensity of the sample; $F_{Standard}$ is fluorescence intensity of the standard; Abs_{sample} is absorbance of the sample at the excitation wavelength; and $Abs_{standard}$ is the absorbance of the standard at the excitation wavelength. The emission spectra of both **Pc-1** and **Pc-2** were measured in different solvents and corresponding quantum yield data were presented in table 1. From the table 1 data it is apparent that as the polarity of the solvent increases, the emission maxima slightly blue shifted by 3-5 nm and quantum yield is reduced in both phthalocyanines. This might be due to the increase of aggregation in polar solvents, which reduces the possibility of radiative deactivation *i.e.*, fluorescence through dissipation of energy by the aggregates.[57] The quantum yields are greatly reduced in un-substituted phthalocyanines. This in turn effect on the singlet excited life time. Figure 6 shows the fluorescence decay signals of both phthalocyanines in CH_2Cl_2 solvent. The lifetimes (radiative) of both phthalocyanines were measured in different solvents and corresponding data are presented in table 1. As in steady state emission, lifetimes were also affected with polarity of the solvents used.

Table 1 Absorption, emission data of **Pc-1** & **Pc-2** in different solvents.

Sample	Solvent	λ_{max}, nm (log ε) $M^{-1}cm^{-1}$	$\lambda_{em.\ max.}$ nm	ϕ_f	τ_f (ns)
Pc-1	Toluene	688 (4.85)	696	0.32	2.73
	DCM	690 (4.76)[a]	696	0.31	2.60
	THF	682 (4.64)	691	0.29	2.97
	DMF	686 (4.61)	695	0.28	2.40
	DMSO	688 (4.59)	698	0.26	2.50
Pc-2	Toluene	685 (4.84)	693	0.27	2.81
	DCM	684 (4.56)[b]	691	0.26	2.70
	THF	680 (4.37)	689	0.25	3.18
	DMF	682 (4.19)	691	0.24	2.60
	DMSO	685 (4.14)	693	0.22	2.91

a log ε value is recorded for DCM only
b log ε value is recorded for DCM only

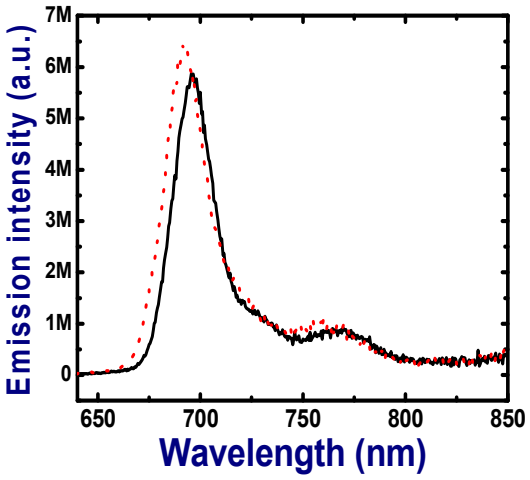

Fig. 5 Emission spectrum of **Pc-1** (–) & **Pc-2** (----) in DCM at λ_{exc} = 680 nm.

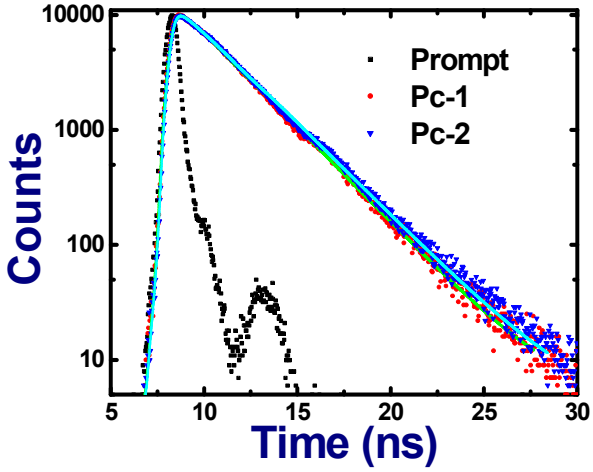

Fig. 6 Fluorescence decay signals of **Pc-1** & **Pc-2** in DCM. The detection wavelength was at 690 nm. Solid line is a fit to the experimental data

Table 2 Half wave potential (V vs SCE) of **Pc-1** & **Pc-2** in DCM, 0.1 M TBAP

Compound	Oxidation		Reduction		ΔE1/2 (V)[a]
Pc-1	0.65,	1.52	-0.96	-1.32	1.61
Pc-2	0.50,	1.22	-0.92	-1.22	1.42

[a] HOMO-LUMO gap (potential difference between the first oxidation and first reduction)

NLO Results and Discussion

Figures 7a-d illustrate the open aperture data of **Pc-1** obtained using ~1.5ps pulses at wavelengths of 640 nm, 680 nm, 700 nm, and 800 nm, respectively. Typical peak intensities used were ~60 GW/cm^2. In all the figures open, black circles represent the experimental data while the solid, red lines represent the theoretical fits. Below 700 nm we did observe strong linear absorption for **Pc-1** and, therefore, nonlinear absorption mechanism was more of saturable absorption (SA) type. However, at 800 nm we do see reverse saturable absorption (RSA) and this is due to the absence of any linear absorption and associated large peak intensities leading to an effective 2PA (either 1+1 or instantaneous two-photon absorption). Solvent (DCM) contribution in the present case is neglected since no transmittance change was observed when the Z-scan was performed with solvent alone. Independent intensity dependent measurements confirmed the dominance of instantaneous 2PA. However, there could be minor contribution from 1+1 type of 2PA.

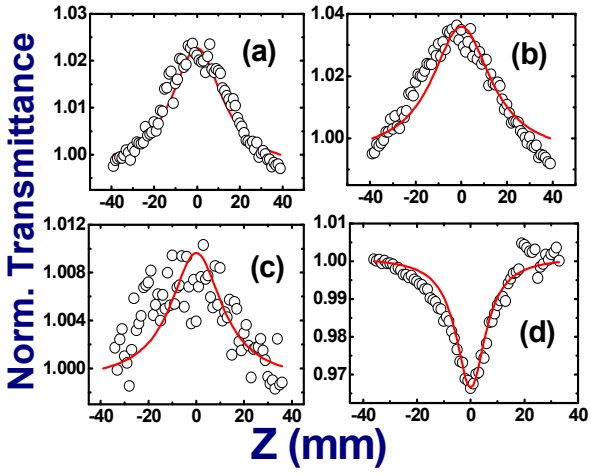

Fig. 7 Ps open aperture Z-scan data of **Pc-1** showing SA at (a) 640 nm (b) 680 nm and (c) 700 nm and RSA at (d) 800 nm. **Pc-1** shows RSA for 800 nm. The peak intensities used were ~60 GW/cm^2. Solid lines are theoretical fits to the experimental data.

Figures 8a-d depict the closed aperture data for **Pc-1** at 640 nm, 680 nm, 700 nm, and 800 nm, respectively. All the data exhibited negative type of nonlinearity with magnitudes in the range of 1.5-7.1×10^{-16} cm^2/W. The solvent contribution again was minimal. The peak intensities used for closed aperture data were typically ~25 GW/cm^2. The asymmetry in figures 9a and 9c could be due to the poor spatial beam profile. Figures 9a-d illustrates the open aperture data of **Pc-2** recorded at wavelengths of 640 nm, 680 nm, 700 nm, and 800 nm, respectively. It is evident that except at 700 nm we observed RSA for the peak intensities used and the data fitted well for 2PA. At 700 nm, though, we observed SA and this can be explained from the linear absorption spectra which indicated a strong absorption peak near 700 nm. However, harder pumping could lead to 2PA/ESA as was observed in some of our earlier studies.[58-64] Tables 3 and 4 summarize the NLO coefficients extracted from various fits to the data for both **Pc-1** and **Pc-2**. Figures of merit were also evaluated for these molecules and they were found to be comparable with some of the recently, successfully reported organic molecules.[58-64]

Table 3 Summary of NLO coefficients of **Pc-1** recorded with ~1.5 ps pulses

λ (nm)	n_2 (cm^2/W)	β (cm/W)	σ_2 (GM)	$\lvert Re[\chi^{(3)}] \rvert$	$\lvert Im[(\chi^{(3)})] \rvert$	Total$[\chi^{(3)}]$	FOM (W)
640	-2.1×10^{-16}	$*\ 0.2\times10^{-11}$	-	1.1×10^{-14}	4.7×10^{-16}	1.1×10^{-14}	0.39
680	-1.5×10^{-16}	$*\ 0.4\times10^{-11}$	-	7.7×10^{-15}	10×10^{-16}	7.8×10^{-15}	0.23
700	-3.3×10^{-16}	$*\ 0.2\times10^{-11}$	-	1.7×10^{-14}	6.4×10^{-16}	1.7×10^{-14}	0.47
800	-7.1×10^{-16}	1.6×10^{-11}	3297	3.6×10^{-14}	5.2×10^{-15}	3.7×10^{-14}	0.70

* sign of β indicates the presence of saturable absorption (SA). $\chi^{(3)}$ values are reported in e.s.u.

Table 4 Summary of NLO coefficients of **Pc-2** recorded with ~1.5 ps pulses

λ (nm)	n_2 (cm^2/W)	β (cm/W)	σ_2 (GM)	$\lvert Re[\chi^{(3)}] \rvert$	$\lvert Im[(\chi^{(3)})] \rvert$	Total$[\chi^{(3)}]$	FOM (W)
640	5.4×10^{-16}	2.3×10^{-11}	5925	2.8×10^{-14}	6.0×10^{-15}	2.8×10^{-14}	1.03
680	-2.4×10^{-16}	2.2×10^{-11}	5325	1.2×10^{-14}	6.0×10^{-15}	1.4×10^{-14}	0.38
700	0.6×10^{-16}	$*\ 0.05\times10^{-11}$	-	3.1×10^{-15}	1.4×10^{-16}	3.1×10^{-15}	0.08
800	-2.4×10^{-16}	6.5×10^{-11}	13395	1.2×10^{-14}	2.1×10^{-14}	2.5×10^{-14}	0.23

* sign in β indicates the presence of saturable absorption (SA). $\chi^{(3)}$ values are reported in e.s.u.

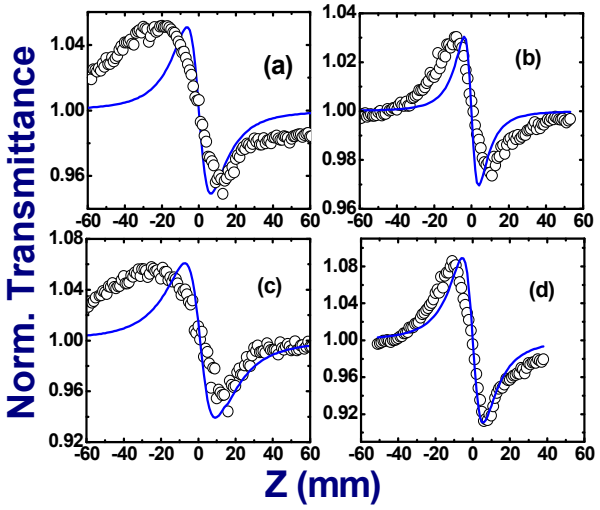

Fig. 8 Ps closed aperture Z-scan data of **Pc-1** showing negative nonlinearity at (a) 640 nm (b) 680 nm (c) 700 nm and (d) 800 nm. The peak intensities used were ~25 GW/cm^2. Solid lines are theoretical fits to the experimental data.

Figures 10a-d demonstrate the closed aperture Z-scan data of **Pc-2** obtained at all the four wavelengths where open aperture data was recorded. Interestingly, the sign of nonlinearity was positive at 680 nm, and 700 nm whereas the sign was negative at 640 nm and 800 nm. We further investigated the NLO properties of these molecules using fs pulses (~140 fs duration at 80 MHz). Figures 11a-d depicts the open aperture data obtained for both **Pc-1** and **Pc-2**. Figure 11a depicts the nonlinear absorption behavior (data fitted again with 2PA) for fs pulse excitation with ~35 mW average input power. The behavior was similar when excited with 1 kHz chopped pulses and at 760 nm, the data of which is presented in figure 11b for **Pc-1**. However, the behavior of **Pc-2** was found to different with SA obtained at similar average powers for both 80 MHz and 1 kHz excitation and the data is presented in figure 11c and 11d, respectively. Typical peak intensities used in this case were in the range of 10^8-10^9W/cm^2. The observed behavior, again, can be attributed to the linear absorption. The different between fs and ps excitation is the spectral bandwidths associated with the pulses. In the fs case the bandwidth was ~9-10 nm (FWHM) whereas with ps excitation the bandwidth was ~1 nm. Therefore, with fs excitation we observed SA even at 800 nm, probably, due to the residual absorption resulting from the weak absorption peak near 800 nm (see figures 13a, 13b of SI for DCM).

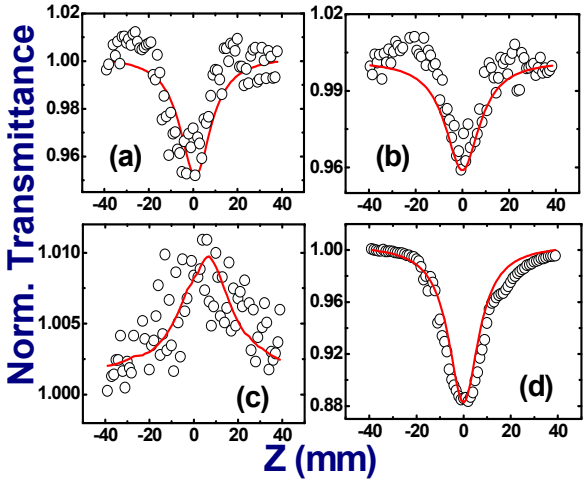

Fig. 9 Ps open aperture Z-scan data of **Pc-2** shows RSA at (a) 640 nm (b) 680 nm and (d) 800 nm and SA at (c) 700 nm. At 700 nm PC-2 shows maximum linear absorption and SA. The peak intensities used were ~60 GW/cm^2. Solid lines are theoretical fits to the experimental data.

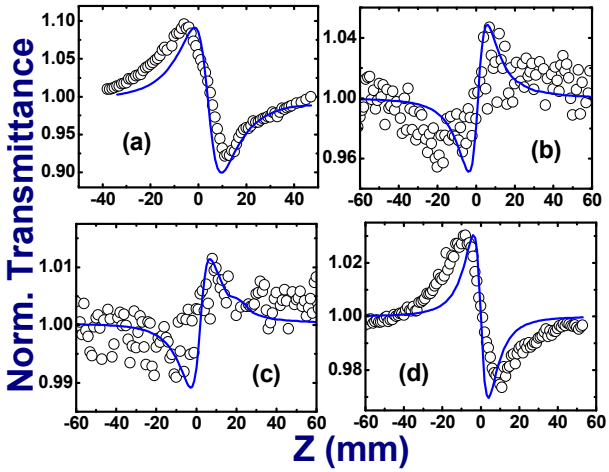

Fig. 10 Ps closed aperture Z-scan data of **Pc-2** (a) 640 nm (negative n_2) (b) 680 nm (positive n_2) (c) 700 nm (positive n_2) (d) 800 nm (negative n_2). The peak intensities used were ~25 GW/cm^2. Solid lines are theoretical fits to the experimental data.

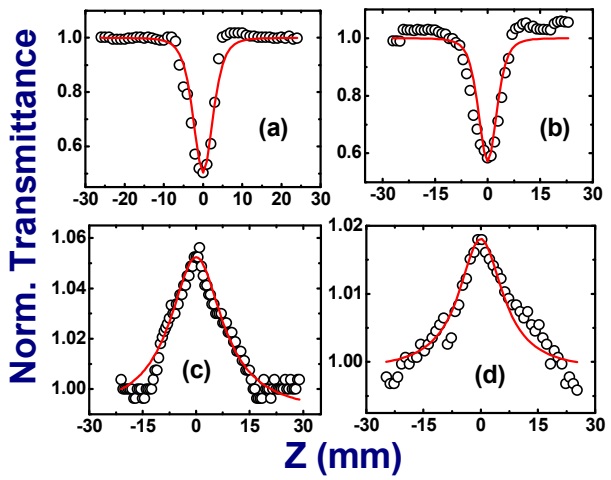

Fig 11 Fs open aperture Z-scan data shows 2PA for **Pc-1** (a) 800 nm, 80 MHz, 35 mW (b) 760 nm, 1 kHz, 30 mW. SA observed for fs open aperture data of **Pc-2** (c) 800 nm, 32 mW, 80 MHz (d) 800 nm, 12 mW, 1 kHz. Typical peak intensities used were 10^8-10^9 W/cm^2. Solid lines are theoretical fits to the experimental data

However, in the ps case due to large peak intensities associated with the focused pulses (an order of magnitude higher than those used in the fs case) 2PA probably dominated over linear absorption. We do expect a switchover from SA to RSA kind of behavior with stronger pumping (higher peak intensities) in the fs case.

The only difference between the chemical structures of Pc-1 and Pc-2 is the peripheral groups attached [3,4-dimethoxy phenyl group in the case of **Pc-1** and 2,6-dimethoxy phenyl **Pc-2**]. The NLO coefficients obtained were significantly different even with this slight difference. 2PA cross-sections (σ_2)/coefficients (β) presented in tables 3 and 4 clearly suggest that the highest σ_2/β values were obtained at 800 nm for both these molecules. Pc-2 σ_2/β value was ~4 times higher than that of Pc-1 σ_2 value and this could possibly be attributed to the higher linear absorption in Pc-1 at 800 nm compared to Pc-2. Furthermore, at 800 nm the n_2 value of Pc-1 was found to be higher than n_2 value of Pc-2 (~3 times stronger). The maximum value of $\chi^{(3)}$ was observed at 800 nm for both the molecules. However, $\chi^{(3)}$ of Pc-2 was of similar magnitude (~10^{-14} e.s.u) to that of Pc-1. The values of n_2 obtained in Pc-1 and Pc-2 were an order of magnitude lower than that of unsymmetrical alkoxy and alkyl substituted Zinc phthalocyanines[46] and a symmetrical Zinc phthalocyanine[31] which were investigated earlier by our group. At 700 nm the β value of Pc-1 was lower than that of Pc-2. However, at 640 nm and 680 nm Pc-2 had stronger nonlinear absorption coefficients compared to Pc-1. For the case of n_2 Pc-2 had positive nonlinearity at 640 nm and 700 nm whereas Pc-1 had negative nonlinearity, which requires further investigations. The magnitudes of n_2, though, were similar in the case of Pc-1 and Pc-2

We had earlier performed detailed studies on a variety of phthalocyanines using cw, ns, ps, and fs pulses. We had investigated (a) alkoxy and alkyl phthalocyanines[9,25-28,30,46] using cw, ns, ps, and fs pulses (b) phthalocyanine thin films[32] using ps pulses (c) phthalocyanine nanoparticles[29] using ns and fs pulses (d) symmetrical and unsymmetrical phthalocyanines[31] using ps pulses for evaluating their NLO properties. The summary of our meticulous NLO studies performed earlier on different phthalocyanines is as follows: (a) Unsymmetrical phthalocyanines had superior NLO properties compared to symmetrical counterparts. It has been established that the optical nonlinearity of a molecule increases with asymmetry if the excited states transition moments dominate (b) Alkoxy phthalocyanines had improved NLO properties compared to alkyl counterparts (c) Thin films possessed superior NLO properties compared to solutions (d) Nanoparticles demonstrated enhanced NLO properties compared to bulk solutions (e) Metal phthalocyanines NLO performance was superior to free-base phthalocyanines. The experimental data from these studies clearly advocate that (i) doping these molecules in thin transparent polymer films (ii) creating nanoparticles from these phthalocyanines (c) performing an unsymmetrical substitution (d) inserting a heavier metal could enhance the NLO properties further.

The data analysis clearly proposes that using the same molecule one could achieve SA, RSA, or RSA in SA using different methodologies such as (a) same wavelength excitation but different pulse width excitation (b) same pulse width excitation but at different input wavelengths. Furthermore, one could easily tune the nonlinear absorption mechanism by slightly changing the peripheral substitutions of a phthalocyanine molecule. In our earlier studies we observed three-photon absorption (3PA) in alkyl and alkoxy phthalocyanines with ~100 fs pulse excitation.[9] In these set of molecules also one could possibly achieve 3PA when pumped with higher peak intensities. The NLO coefficients (β) recorded in Pc-1 and Pc-2 are superior to that of alkoxy phthalocyanines studied earlier by our group.[27] That these molecules do not aggregate even at higher concentrations combined with the strong NLO coefficients make them potential candidates for photonic applications. In the case of aggregation the energy level structure is generally modified thereby altering the optical and NLO properties and furthermore aggregation effects are not desirable for most of the device applications. Complete details of the experimental setup, equations used for fitting the experimental data (SA/2PA) for both fs 80 MHz and 1 kHz excitations is presented in supporting information.

Pump-probe studies

Figure 12 shows the degenerate pump-probe data of **Pc-1** and **Pc-2** (in DCM) obtained near 600 nm using ~70 fs pulses with typical pump energies of 10 μJ. Details of the experimental setup can be found in our earlier works.[59-61] Positive $\Delta T/T$ in the pump-probe data indicted photo-bleaching was observed. The data was fitted for a double exponential and two lifetimes (τ_1 and τ_2) were retrieved from each of the fits. The values of τ_1 and τ_2 were ~3 ps and ~40 ps for **Pc-1** whereas the values were ~2 ps and ~500 ps for **Pc-2**. Figure 13 shows a simplified energy level diagram indicating the excitations and decay times for these molecules. Excitation with focused 600 nm photons (16600 cm^{-1}) and the peak intensities used enables 2PA resulting in population reaching the S_2 states. Once excited into the high lying states of S_2 the de-excitation mechanism could be from (a) lowest vibrational state of S_2 manifold to highest vibrational states of S_1 manifold (Internal Conversion, IC) followed by intra-molecular vibrational relaxation (IVR) from highest states of S_1 to lowest states of S_1).

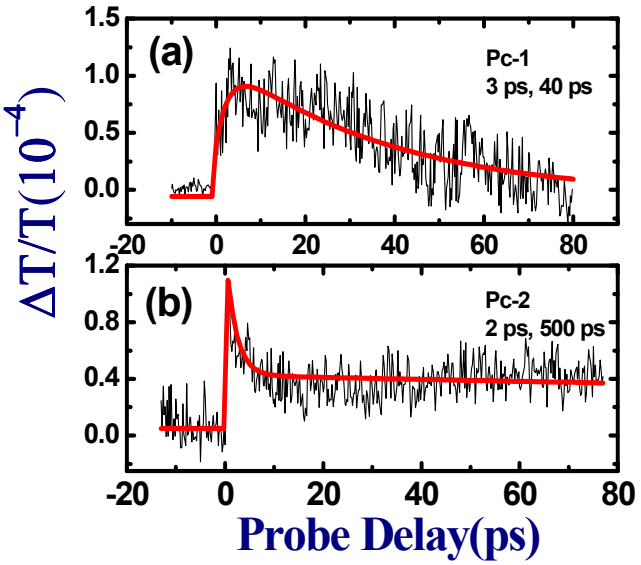

Figure 12 Degenerate pump-probe data of (a) **Pc-1** and (b) **Pc-2** obtained

with ~70 fs pulses near 600 nm. Solid lines are theoretical fits to the experimental data (wriggly lines).

These are typically fast processes (<1 ps for IC, 1–2 ps for IVR) and, therefore, the shorter lifetimes (2–3 ps) could be attributed to this relaxation and (b) from the lowest vibrational states of S_1 states the molecules relax to ground state via non-radiative mechanism by releasing the energy to solvent. This process typically occurs in few tens to hundreds of ps in such molecules. The longer lifetime can be associated with such a process as depicted in fig 13. The longer lifetime cannot be due to radiative processes since the radiative lifetimes measured in different solvents were typically few ns.[39] The lifetimes observed in Pc-1 and Pc-2 were comparable to those obtained in similar molecules such as Porphycenes[59], Corroles[60], Naphthobipyrroles,[61] which were recently investigated by our group. Pc-1 has a short-lived non-radiative lifetime from S_1 states whereas Pc-2 has a long-lived lifetime. However, the radiative lifetimes of both Pc-1 and Pc-2 were similar in magnitude (2-3 ns). The long-lived lifetime could, possibly, have played a role in the observation of stronger NLO coefficients for Pc-2. We are in the process of modeling the nonlinear absorption of such phthalocyanines using a comprehensive five-level model to account for all the excited state absorptions, 2PA, inter-system crossing rate and singlet/triplet states lifetimes to completely investigate, understand the role of excited states in enhancement of NLO coefficients.

We strongly believe that the present work extracted the potential of these molecules for photonic applications and further studies in the direction of implementing NLO studies after doping these materials in appropriate matrices will further enhance their potential. To the best of our knowledge these are first of its kind studies wherein both ps and fs optical nonlinearities along with excited state dynamics of phthalocyanines have been evaluated. Our future efforts will be directed towards (a) exploring the optical limiting capabilities of these molecules with ns pulses and (b) investigating the ultrafast near-IR nonlinearities using degenerate four wave mixing techniques.

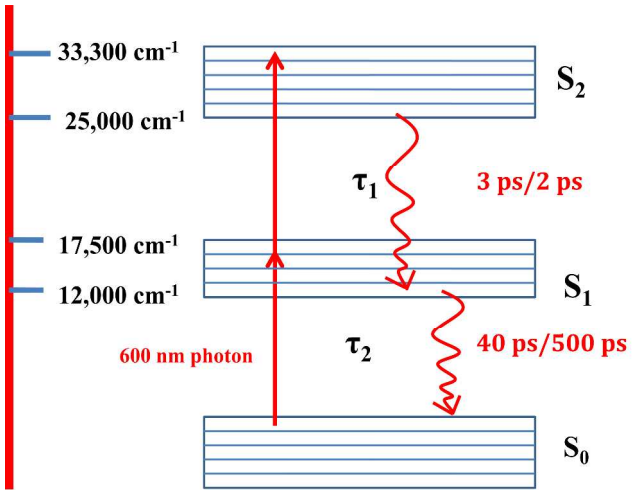

Fig. 13 Typical energy level diagram of **Pc-1** and **Pc-2**.

Conclusions

In summary two novel sterically hindered phthalocyanines were synthesized and characterized. Their optical and electrochemical properties have been investigated in detail. Nonlinear optical (NLO) properties were also evaluated at different in the visible spectra region using picosecond (~1.5 ps) pulses and further studies with femtosecond (~140 fs) pulses at 800 nm have been performed. 2PA and saturable absorption were the dominant nonlinear asorption mechanmisms observed with ps excitation while 2PA was observed with fs excitation. NLO coefficients were extracted from ps/fs closed and open aperture Z-scan measurements at different wavelengths of visible spectra regime. Large two-photon absorption cross sections in the range of ~14000 GM and n_2 values in the range of 1-7×10^{-16} cm^2/W were recorded for these samples. The largest σ_2/β values were obtained at 800 nm for both these molecules. Pc-2 σ_2 value was ~4 times higher than that of Pc-1 σ_2 value. Furthermore, at 800 nm the n_2 value of Pc-1 was found to be higher than n_2 value of Pc-2 (~3 times stronger). The values of n_2 obtained in Pc-1 and Pc-2 were an order of magnitude lower than that of unsymmetrical alkoxy and alkyl substituted Zinc phthalocyanines[46] and a symmetrical Zinc phthalocyanine[31] which were investigated earlier by our group. For the case of n_2 Pc-2 had positive nonlinearity at 640 nm and 700 nm whereas Pc-1 had negative nonlinearity. The excited state decay dynamics were investigated using degenerate pump-probe experiments with femtosecond pulses near 600 nm. Double exponential fits of the pump-probe data suggested two decay times. The shorter lifetime was 2-3 ps while the longer lifetime was ~40 ps in **Pc-1** and ~500 ps in **Pc-2**. Our studies suggest that these molecules can be tailored for potential applictions in photonics.

Acknowledgments

SVR and DS thank DRDO for continued financial support. LG thanks to CSIR-XII FYP '*Intel Coat*' project CSC-0114. VKS and NVK thanks to CSIR for research fellowships.

References

1. A.B. Sorokin, *Acc. Chem. Res*. 2013, dx.doi.org/10.1021/cr4000072
2. L. Giribabu, R. K. Kanaparthi and V. Velkannan, *The Chem. Record* 2012, **12**, 306.
3. Z. Sun, L. Jin, S. He, Y. Zhao, M. Wei, D. G. Evans and X. Duan, *Green Chem*. 2012, **14**, 1909.
4. S. Nagel, M. Lerner, C. Keil, R. Gerdes, L. Lapok, S. M. Gorun and D. Schlettwein, *J. Phys. Chem. C* 2011, **115**, 8759.
5. T. Nyokong, *Pure Appl. Chem*. 2011, **83**, 1763.
6. G. de la Torre, P. Vázquez, F. Agulló-López and T. Torres, *Chem. Rev*. 2004, **104**, 3723.
7. Y. H. Gursel, B. F. Senkal, M. Kandaz and F. Yakuphanoglu, Polyhedron 2009, **28**, 1490.
8. C. G. Claessens, U. Hahn and T. Torres, *The Chem. Record* 2008, **8**, 75.
9. R.S.S. Kumar, S. Venugopal Rao, L. Giribabu and D. Narayana Rao, *Chem. Phys. Lett*. 2007, **447**, 274.
10. P. Gregory, *J. Porphy. Phth*. 2000, **4**, 432.
11. K.M. Smith, in: A.R. Katritzky, C.W. Rees (Eds.), *Comp. Heter. Chem.,* vol. 4, Pergamon, Oxford, 1984, pp. 377–442.
12. J. Simon and J. Vacus, *Adv. Mater*. 1995, **7**, 797.
13. E. M. Maya, A. W. Snow, J. S. Shirk, R. G. S. Pong, S. R. Flom and G. L. Roberts, *J. Mater. Chem*. 2003, **13**, 1603.
14. I. Szymczyk and H. Abramczyk, *Pure Appl. Chem.* 2004, **76**, 183.
15. K. M. Kadish, K. M. Smith, R. Guilard, The Porphyrin Handbook, Academic Press, San Diego, CA, 2003, Vol 17: Phthalocyanines: Properties and Materials.
16. M. Brewis, B.M. Hassan, H. Li, S. Makhseed, N.B. McKeown and N. Thompson, *J. Porphyrins& Phthalocyanines* 2000, 4, 460.
17. M. Brewis, G.J. Clarkson, A.M. Holder and N.B. McKeown, *Chem. Commun*. 1998, 969.
18. L. Giribabu, R.K. Kanaparthi, *Curr. Sci*. 2013, **104**, 847.
19. L. Giribabu, V.K. Singh, T. Jella, Y. Soujanya, A. Amat, F. De Angelis, A. Yella, P. Gao, M.K. Nazeeruddin, *Dyes and Pigments* 2013, **98**, 518.
20. L. Giribabu, V. K. Singh, Ch. V. Kumar, Y. Soujanya, P. Y. Reddy, M. L. Kantam, *Solar Energy*, 2011, **85**, 1204.
21. P.Y. Reddy, L. Giribabu, C. Lyness, H. J. Snaith, Ch. Vijaykumar, M. Chendrasekheram, M. L. Kantam, J. Hum, K. Kalyanasundaram, M. Gratzel and M. K.Nazeeruddin, *Angew. Chem. Int. Ed. Eng*., 2007, **46**, 373.
22. L. Giribabu, Ch. Vijaykumar, V. G. Reddy, P. Y. Reddy, S.-R. Jang, J.-H. Yum, M. K. Nazeeruddin and M. Gratzel, *Solar Energy Mater. Solar Cells*, 2007, **91**, 1611.
23. S. Eu,T. Katoh,T. Umeyama,Y. Matanoand H. Imahori, *Dalton Trans.*, 2008, 5476.
24. G. Pozzi, S. Quici, M.C. Raffo, C.A. Bignozzi, S. Caramori and M. Orlandi, *J. Phys. Chem. C* 2011, **115**, 3777.

25. S.J. Mathews, S. Chaitanya Kumar, L. Giribabu, S. Venugopal Rao, *Opt. Commun.* 2007, **280**, 206.
26. S.J. Mathews, S. Chaitanya Kumar, L. Giribabu, S. Venugopal Rao, *Mater. Lett.* 2007, **61**, 4426.
27. N. Venkatram, L. Giribabu, D. Narayana Rao, S. Venugopal Rao, *Chem. Phys. Lett.* 2008, **464**, 211.
28. N. Venkatram, L. Giribabu, D. Narayana Rao, S. Venugopal Rao, *Appl. Phys. B* 2008, **91**, 149.
29. S. Venugopal Rao, L. Giribabu, N. Venkatram, D. Narayana Rao, *J. Appl. Phys.* 2009, **105**, 053109.
30. R.S.S. Kumar, S. Venugopal Rao, L. Giribabu, D. Narayana Rao, *Opt. Mat.,* 2009, **31**, 1042.
31. S. Venugopal Rao, P.T. Anusha, L. Giribabu, Surya P. Tewari, *Pramana - J. Phys.*, 2010, **75**, 1017.
32. S. Venugopal Rao, P.T. Anusha, T.S. Prashant, Debasis Swain, Surya P. Tewari, *Mater. Sci. Applns.,* 2011, **2**, 299.
33. X. Zhao, X.-Q. Yan, Q. Ma, J. Yao, X.-L. Zhang, Z.-B. Liu, J.-G. Tian, *Chem. Phys. Lett.* 2013, **577**, 62.
34. S. Tekin, U. Kürüm, M. Durmuş, H.G. Yaglioglu, T. Nyokong, A. Elmali, *Opt. Commun.* 2010, **283**, 4749.
35. C. Yao, Y. Zhang, W. Sun, C. Yu, J. Li, and P. Yuan, *Opt. Express* 2013, **21**, 2212.
36. H. Gu, S. Li, J. Wang, W.J. Blau, Y. Chen, *Mater. Chem. Phys.* 2012, **137**, 188.
37. A.B. Karpo, V.E. Pushkarev, V.I. Krasovskii, L.G. Tomilova, *Chem. Phys. Lett.* 2012, **554**, 155.
38. H. Manaa, A. Tuhl, J. Samuel, A. Al-Mulla, N.A. Al-Awadi, S. Makhseed, *Opt. Commun.* 2011, **284**, 450.
39. Y. Chen, S.M. O'Flaherty, M. Hanack, W.J. Blau, *J. Mater. Chem.* 2203, **13**, 2405.
40. E.M. Maya, A.W. Snow, J.S. Shirk, R.G.S. Pong, S.R. Flom, G.L. Roberts, *J. Mater. Chem.* 2003, **13**, 1603.
41. A. Auger, W.J. Blau, P.M. Burnham, I. Chambrier, M.J. Cook, B. Isare, F. Nekelson, S.M. O'Flaherty, *J. Mater. Chem.* 2003, **13**, 1042.
42. A. Tuhl, H. Manaa, S. Makhseed, N. Al-Awadi, J. Mathew, H.M. Ibrahim, T. Nyokong, H. Behbehani, *Opt. Mater.* 2012, **34**, 1869.
43. W. L. F. Armango, Ch. L. L. Chai, Editors. Purification of laboratory chemicals. NewYork: Butterworth Heinemann; 2003.
44. D. S. Lawrence, D. G. Whitten, *Photochem. Photobiol*. 1996, **64**, 923.
45. M. Sheik Bahae, A.A. Said, T.H. Wei, D.J. Hagan, E.W. Van Stryland, *IEEE J Quant. Electron*. 1990, **26**, 760.
46. P.T. Anusha, P.S. Reeta, L. Giribabu, S.P. Tewari, S. Venugopal Rao, *Mater. Lett.* 2010, **6**, 1915.
47. K.V. Saravanan, K.C. James Raju, M.G. Krishna, S.P. Tewari, S. Venugopal Rao, *Appl. Phys. Lett.* 2010, **96**, 232905.
48. G.K. Podagatlapalli, S. Hamad, S. Sreedhar, S.P. Tewari, S. Venugopal Rao, *Chem. Phys. Lett.* 2012, **530**, 93.
49. S. Venugopal Rao, *J. Mod. Opt.* 2011, **58**, 1024.
50. N. Miyaura, K. Yamada and A. Suzuki, *Tetrahedron Lett*. 1979, **20**, 3437.
51. T. Goslinski, T. Osmalek, K. Konopka, M. Wierzchowski, P. Fita, J. Mielcarek Polyhedron *2011*, **30**, 1538.
52. A. Giraudeau, F. F. Fan and A. J. Bard, *J. Am. Chem. Soc*., 1980, **102**, 5137.
53. B. Simicglavaski, S. Zecevic, E. Yeager. *J ElectrochemSoc* 1987, **134**, C130.
54. B. Agboola, K. I. Ozoemena, T. Nyokong. *Electrochim Acta* 2006, **51**, 4379.
55. Z. Ou, Z. Jiang, N. Chen, J. Huang, J. Shen, K. M. Kadish, *J. Porphy. Phth.* 2008, **12**, 1123.
56. J.B. Birks, Photophysics of Aromatic Molecules, 1st ed., Wiley Monographs in Chemical Physics, Wiley-Interscience, London, 1970.
57. A. Ogunsipe, D. Maree, T. Nyokong. *J. Mol. Strut*. 2003, **650**, 131.
58. T. Sarma, P.K. Panda, P.T. Anusha, S. Venugopal Rao, *Org. Lett.* 2010, **13**, 188.
59. D. Swain, P.T. Anusha, T.S. Prashant, S.P. Tewari, T. Sarma, P.K. Panda, S. Venugopal Rao, *Appl. Phys. Lett.* 2012, **100**, 141109.
60. P.T. Anusha, D. Swain, S. Hamad, L. Giribabu, T.S. Prashant, S.P. Tewari, S. Venugopal Rao, *J. Phys. Chem. C* 2012, **116**, 17828.
61. D. Swain, T. Sarma, P.K. Panda, S. Venugopal Rao, *Chem. Phys. Lett.* 2013, **580**, 73.
62. S. Hamad, Surya P. Tewari, L. Giribabu, S. Venugopal Rao, *J. Porphy. Phth.* 2012, **16**, 140.
63. B.S. Singh, H.R. Lobo, G.K. Podagatlapalli, S. Venugopal Rao, G.S. Shankarling, *Opt. Mater.* 2013, **35**, 962.
64. E.D. D'Silva, G. Krishna Podagatlapalli, S. Venugopal Rao, S.M. Dharma Prakash, *Mater. Res. Bull.* 2012, **47,** 3552.